The f_2- and ρ_3-mesons in multi-channel pion-pion scattering

Yu.S. Surovtsev[*]

Bogoliubov Laboratory of Theoretical Physics, JINR, Dubna 141980, Russia

P. Bydžovský[†]

Nuclear Physics Institute, ASCR, Řež near Prague 25068, Czech Republic

R. Kamiński[‡]

Institute of Nuclear Physics, PAN, Cracow 31342, Poland

M. Nagy[§]

Inst. Phys. Slovak Acad. Sci., Dubravska cesta 9, 845 11 Bratislava, Slovak Republic

(Dated: April 5, 2011)

Abstract

In a multi-channel S-matrix approach, data on $\pi\pi \to \pi\pi, K\overline{K}, \eta\eta$ in the $I^G J^{PC} = 0^+ 2^{++}$ sector and $\pi\pi$ scattering in the $1^+ 3^{--}$ sector are analyzed to study the f_2- and ρ_3-mesons, respectively. Spectroscopic implications and possible classification of the f_2-states in terms of the SU(3) multiplets are also discussed.

PACS numbers: 11.55.Bq, 13.75.Lb, 14.40.Cs

---

[*] E-mail address: surovcev@theor.jinr.ru

[†] E-mail address: bydz@ujf.cas.cz

[‡] E-mail address: Robert.Kaminski@ifj.edu.pl

[§] E-mail address: fyzinami@unix.savba.sk

I. INTRODUCTION

We present results of the coupled-channel analysis of data on processes $\pi\pi \to \pi\pi, K\overline{K}, \eta\eta$ in the $I^G J^{PC} = 0^+ 2^{++}$ sector and on the $\pi\pi$ scattering in the $1^+ 3^{--}$ sector.

Our knowledge about the existence and parameters of resonances in the $0^+ 2^{++}$ sector is not clear yet. Nine from the thirteen resonances, discussed in the PDG issue [1] and in the literature [2], $f_2(1430)$, $f_2(1565)$, $f_2(1640)$, $f_2(1810)$, $f_2(1910)$, $f_2(2000)$, $f_2(2020)$, $f_2(2150)$, $f_2(2220)$, must be still confirmed in various experiments and analyses. In the analysis of processes $p\overline{p} \to \pi\pi, \eta\eta, \eta\eta'$ [2] five resonances – $f_2(1920)$, $f_2(2000)$, $f_2(2020)$, $f_2(2240)$ and $f_2(2300)$ – have been obtained, where the $f_2(2000)$ is a candidate for the glueball. In our analysis of $\pi\pi \to \pi\pi, K\overline{K}, \eta\eta$ [3] we supported this conclusion on the $f_2(2000)$.

The tensor sector is also interesting because here multi-quark states might be observed apparently as separate states, which are difficult to observe in the scalar sector where owing to their large widths these states can manifest themselves only in a distortion of the $q\bar{q}$ picture.

Investigation in the $I^G J^{PC} = 1^+ 3^{--}$ sector is motivated by those results [3, 4] in the $0^+ 2^{++}$, $0^+ 0^{++}$ and $1^+ 1^{--}$ sectors, which (if they are confirmed) will require revisions of the mainstream quark models, e.g. [5], and by a possibility to support (or not) these results when studying of other mesonic sectors. These are the earlier obtained disagreements with predictions of the indicated model, e.g., with respect to the $f_0(600)$ and $f_0(1500)$ in the scalar sector and to the second $q\bar{q}$ nonet in the tensor sector [3, 4]. Especially it is worth to remind that result in the vector sector: In our multi-channel analysis [3, 6] of the P-wave $\pi\pi$ scattering data [7] and in the re-analysis of the process $e^+ e^- \to \omega\pi^0$ [8], the old conclusion [9] was confirmed (which, to the point, is consistent with results of some quark models [10]) that the first ρ-like meson is $\rho(1250)$ unlike $\rho(1450)$ cited in the PDG tables [1]. However, existence of both states does not contradict to the $\pi\pi$ scattering data [3, 6]. It is important that for both states there are apparently possible SU(3) partners. For the $\rho(1250)$ these partners are: the isodoublet $K^*(1410)$ and the isoscalar $\omega(1420)$, for which the obtained mass is in range 1350-1460 MeV [1], whereas the Gell-Mann–Okubo (GM-O) formula

$$3m_{\omega_8'}^2 = 4m_{K^{*\prime}}^2 - m_{\rho'}^2$$

gives for the mass of the eighth component of corresponding octet the value about 1460 MeV. The $\rho(1450)$, which might be the isovector $^3D_1$ state in the $q\bar{q}$ picture, could be put into

the octet together with the isodoublet $K^*(1680)$. Then from the GM-O formula, the value 1750 MeV is obtained for the mass of the eighth component of this octet. This corresponds to one of the observations of the second ω-like meson which is cited in the PDG tables under the $\omega(1650)$ and has the mass, obtained in various works, from 1606 to 1840 MeV.

In the mainstream quark model [5], the first ρ-like meson is usually predicted by about 200 MeV higher than the $\rho(1250)$, and also the first K^*-like meson is obtained at 1580 MeV, whereas the corresponding well established resonance has the mass of about 1410 MeV. Therefore, it is important to check if the conclusion on the $\rho(1250)$ is supported by investigation in other mesonic sectors. Considering the (J, M^2)-plot for the daughter ρ-trajectory, related to the suggested $\rho(1250)$, one concludes that there should exist the 1^+3^{--}-state at about 1950 MeV –"$\rho_3(1950)$". It is worth to check this state analyzing accessible data on the F-wave $\pi\pi$ scattering [7].

In the present investigation, we applied the multi-channel S-matrix approach [3]. To generate resonance poles and zeros on the Riemann surface, we used the multi-channel Breit–Wigner forms taking into account the Blatt–Weisskopf barrier factors given by spins of resonances [11].

II.   THE S-MATRIX FORMALISM FOR N COUPLED CHANNELS

The N-channel S-matrix is determined on the 2^N-sheeted Riemann surface. The matrix elements S_{ab} ($a, b = 1, 2, \cdots, N$ denote channels) have the right-hand cuts along the real axis of the complex-s plane (s is the invariant total energy squared), related to the considered channels and starting in the channel thresholds s_i ($i = 1, \cdots, N$), and the left-hand cuts related to the crossed channels. The main model-independent part of resonance contributions is given by poles and zeros on the Riemann surface. Generally, this representation of resonances can be obtained utilizing formulas for the analytic continuations of the matrix elements for the coupled processes to the unphysical sheets of the Riemann surface, as it was performed for the N-channel case in Ref. [12].

In this work, the Le Couteur–Newton relations [13] are used to generate the resonance poles and zeros on the Riemann surface. These relations express the S-matrix elements of all coupled processes in terms of the Jost matrix determinant $d(k_1, \cdots, k_N)$ ($k_i = \frac{1}{2}\sqrt{s - s_i}$)

that is a real analytic function with the only branch-points at $k_i = 0$:

$$S_{aa} = \frac{d(k_1, \cdots, k_{a-1}, -k_a, k_{a+1}, \cdots, k_N)}{d(k_1, \cdots, k_N)},$$

$$S_{aa}S_{bb} - S_{ab}^2 = \frac{d(k_1, \cdots, k_{a-1}, -k_a, k_{a+1}, \cdots, k_{b-1}, -k_b, k_{b+1}, \cdots, k_N)}{d(k_1, \cdots, k_N)}. \qquad (1)$$

The real analyticity implies $\quad d(s^*) = d^*(s) \quad$ for all s. The N-channel unitarity requires

$$|d(k_1, \cdots, -k_a, \cdots, k_N)| \leq |d(k_1, \cdots, k_N)|, \; a = 1, \cdots, N,$$

$$|d(-k_1, \cdots, -k_a, \cdots, -k_N)| = |d(k_1, \cdots, k_a, \cdots, k_N)|$$

to hold for physical values of s.

The d-function is taken in the separable form $\quad d = d_B d_{res}$. The resonance part d_{res} is described using the multi-channel Breit–Wigner forms

$$d_{res}(s) = \prod_r \left[M_r^2 - s - i \sum_{i=1}^{N} \rho_{ri}^{2J+1} R_{ri} f_{ri}^2 \right], \qquad (2)$$

where $\rho_{ri} = 2k_i/\sqrt{M_r^2 - s_i}$, $\quad f_{ri}^2/M_r$ indicates to the partial width of a resonance with mass M_r, and $R_{ri}(s, M_r, s_i, r_{ri})$ are the Blatt–Weisskopf barrier factors with s_i the channel threshold and r_{ri} a radius of the i-channel decay of the state "r".

The background part d_B represents mainly an influence of channels which are not explicitly included. Opening of these channels causes a rise of the corresponding elastic and inelastic phase shifts in d_B

$$d_B = \exp\left[-i \sum_{i=1}^{N} \left(\sqrt{\frac{s - s_i}{s}} \right)^{2J+1} (a_i + ib_i) \right]. \qquad (3)$$

From the formulas of analytic continuation of the matrix elements for the coupled processes to the unphysical sheets of the Riemann surface [12], one can conclude that only on the sheets with the numbers 2^i $(i = 1, \cdots, N)$, i.e. II, IV, VIII, XVI,..., the analytic continuations have the form $\propto 1/S_{ii}^I$ where S_{ii}^I is the S-matrix element on the physical (I) sheet. This means that only on these sheets the pole positions of resonances are at the same points of the s-plane, as the resonance zeros on the physical sheet, i.e., they are not shifted due to the coupling of channels. Therefore, *the resonance parameters should be calculated from the pole positions only on these sheets.*

In the four-channel case, considered below, the Riemann surface is sixteen-sheeted. The sheets II, IV, VIII, and XVI correspond to the following signs of analytic continuations of the

4

quantities $\text{Im}\sqrt{s - s_1}$, $\text{Im}\sqrt{s - s_2}$, $\text{Im}\sqrt{s - s_3}$, and $\text{Im}\sqrt{s - s_4}$: $-+++$, $+-++$, $++-+$, and $+++-$, respectively.

III.   ANALYSIS OF THE $I^G J^{PC} = 0^+ 2^{++}$ SECTOR

In the analysis of data on the isoscalar D-waves of processes $\pi\pi \to \pi\pi, K\overline{K}, \eta\eta$, we have considered explicitly also the channel $(2\pi)(2\pi)$. Therefore, we have applied the four-channel Breit–Wigner form for the resonance part (2) of the function $d(\sqrt{s - s_1}, \sqrt{s - s_2}, \sqrt{s - s_3}, \sqrt{s - s_4})$. The Blatt–Weisskopf barrier factor for a particle with $J = 2$ is

$$R_{ri} = \frac{9 + \frac{3}{4}(\sqrt{M_r^2 - s_i}\ r_{ri})^2 + \frac{1}{16}(\sqrt{M_r^2 - s_i}\ r_{ri})^4}{9 + \frac{3}{4}(\sqrt{s - s_i}\ r_{ri})^2 + \frac{1}{16}(\sqrt{s - s_i}\ r_{ri})^4} \tag{4}$$

with radii 0.943 fm for resonances in all channels, except for $f_2(1270)$ and $f_2(1960)$ for which the radii are (as the results of the analysis): for $f_2(1270)$, 1.498, 0.708 and 0.606 fm in channels $\pi\pi$, $K\overline{K}$ and $\eta\eta$, respectively, and for $f_2(1960)$, 0.296 fm in channel $K\overline{K}$.

The background part (3) has the form

$$d_B = \exp\left[-i \sum_{n=1}^{3} \left(\sqrt{\frac{s - s_n}{s}}\right)^5 (a_n + i b_n)\right], \tag{5}$$

where

$$a_1 = \alpha_{11} + \frac{s - 4m_K^2}{s}\ \alpha_{12}\ \theta(s - 4m_K^2) + \frac{s - s_v}{s}\ \alpha_{10}\ \theta(s - s_v),$$

$$b_n = \beta_n + \frac{s - s_v}{s}\ \gamma_n\ \theta(s - s_v).$$

$s_v \approx 2.274\ \text{GeV}^2$ is a combined threshold of the channels $\eta\eta'$, $\rho\rho$, and $\omega\omega$.

The data for the $\pi\pi$ scattering are taken from an energy-independent analysis by B. Hyams et al. [7]. The data for $\pi\pi \to K\overline{K}, \eta\eta$ are taken from works [14].

A satisfactory description (with the total $\chi^2/\text{NDF} = 161.147/(168 - 65) \approx 1.56$) is obtained both with ten resonances – $f_2(1270)$, $f_2(1430)$, $f_2'(1525)$, $f_2(1580)$, $f_2(1730)$, $f_2(1810)$, $f_2(1960)$, $f_2(2000)$, $f_2(2240)$ and $f_2(2410)$ – and with eleven states when adding one more resonance $f_2(2020)$ which is needed in the combined analysis of data on processes $p\overline{p} \to \pi\pi, \eta\eta, \eta\eta'$ [2]. The description with eleven states is practically the same as that with ten resonances: the total $\chi^2/\text{NDF} = 156.617/(168 - 69) \approx 1.58$.

The parameters of the Breit–Wigner generators of the poles are shown in Table I for the ten-states scenario and in Table II for the eleven-states one.

5

TABLE I: The parameters of the Breit–Wigner forms for 10 f_2-states (in MeV).

State	M_r	f_{r1}	f_{r2}	f_{r3}	f_{r4}
$f_2(1270)$	1275.3±1.8	470.8±5.4	22.4±4.6	201.5±11.4	90.4±4.76
$f_2(1430)$	1450.8±18.7	128.3±45.9	8.2±65	562.3±142	32.7±18.4
$f_2'(1525)$	1535±8.6	28.6±8.3	41.6±160	253.8±78	92.6±11.5
$f_2(1600)$	1601.4±27.5	75.5±19.4	127±199	315±48.6	388.9±27.7
$f_2(1730)$	1723.4±5.7	78.8±43	107.6±76.7	289.5±62.4	460.3±54.6
$f_2(1810)$	1761.8±15.3	129.5±14.4	90.3±90	259±30.7	469.7±22.5
$f_2(1960)$	1962.8±29.3	132.6±22.4	65.4±94	333±61.3	319±42.6
$f_2(2000)$	2017±21.6	143.5±23.3	450.4±221	614±92.6	58.8±24
$f_2(2240)$	2207±44.8	136.4±32.2	166.8±104	551±149	375±114
$f_2(2410)$	2429±31.6	177±47.2	460.8±209	411±196.9	4.5±70.8

The background parameters for the ten-states scenario are: $\alpha_{11} = -0.07805$, $\alpha_{12} = 0.03445$, $\alpha_{10} = -0.2295$, $\beta_1 = -0.0715$, $\gamma_1 = -0.04165$, $\beta_2 = -0.981$, $\gamma_2 = 0.736$, $\beta_3 = -0.5309$, $\gamma_3 = 0.8223$.

TABLE II: The parameters of the Breit–Wigner forms for 11 f_2-states.

State	M_r	f_{r1}	f_{r2}	f_{r3}	f_{r4}
$f_2(1270)$	1276.3±1.8	468.9±5.5	7.2±4.6	201.6±11.6	89.9±4.79
$f_2(1430)$	1450.5±18.8	128.3±45.9	8.2±63	562.3±144	32.7±18.6
$f_2'(1525)$	1534.7±8.6	28.5±8.5	51.6±155	253.9±79	89.5±12.5
$f_2(1600)$	1601.5±27.9	75.5±19.6	127±190	315±50.6	388.9±28.6
$f_2(1730)$	1719.8±6.2	78.8±43	108.6±76.	289.5±62.6	460.3±54.5
$f_2(1810)$	1760±17.6	129.5±14.8	90.3±89.5	259±32	469.7±25.2
$f_2(1960)$	1962.2±29.8	132.6±23.3	62.4±91.3	331±61.5	319±42.8
$f_2(2000)$	2006±22.7	155.7±24.4	574.8±211	169.5±95.3	60.4±26.7
$f_2(2020)$	2027±25.6	50.4±24.8	128±190	441±196.7	58±50.8
$f_2(2240)$	2202±45.4	133.4±32.6	168.8±103	545±150.4	381±116
$f_2(2410)$	2387±33.3	175±48.3	462.8±211	395±197.7	24.5±68.5

The background parameters for the eleven-states case are: $\alpha_{11} = -0.0755$, $\alpha_{12} = 0.0225$, $\alpha_{10} = -0.2344$, $\beta_1 = -0.0782$, $\gamma_1 = -0.05215$, $\beta_2 = -0.985$, $\gamma_2 = 0.7494$, $\beta_3 = -0.5162$, $\gamma_3 = 0.786$.

In the following we consider the eleven-states scenario (see discussion in Section V). In Figures 1 and 2 we demonstrate obtained energy dependences of the analyzed quantities, compared with the experimental data.
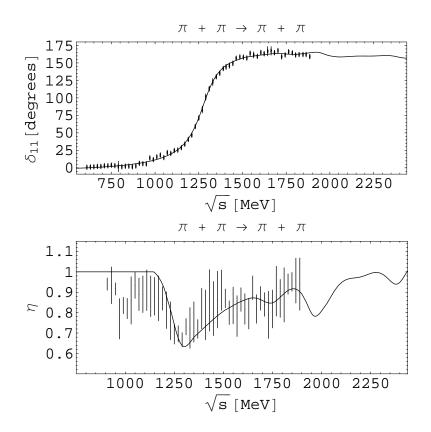

FIG. 1: The phase shift and module of the D-wave $\pi\pi$-scattering S-matrix element.

In Table III we show the poles in the complex energy plane $\sqrt{s}$ (obtained using eqs.(2) and (4)), which must be used for the calculation of the masses and widths of resonances.

Errors of the pole positions shown in Table III are estimated using a Monte Carlo method. In this method, the parameters M_r and f_{rj} are randomly generated using a normal distribution (Gaussian) with the width given by the parameter error in Table II. Having generated the parameters, distributions (histograms for deviations of the pole positions) for the real and imaginary parts of the pole positions are evaluated and the standard deviations, which characterize "widths" of the distributions for the pole position, are calculated.

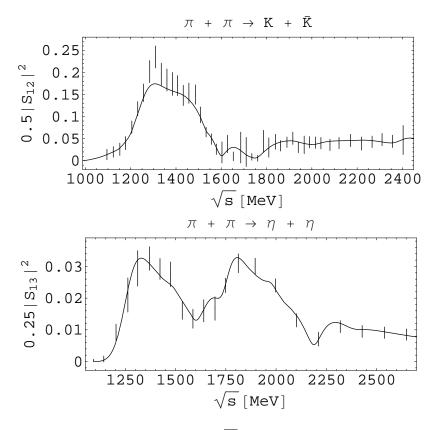The masses m_{res} and total widths Γ_{tot} of states are calculated from the pole positions

FIG. 2: The squared modules of the $\pi\pi \to K\overline{K}$ and $\pi\pi \to \eta\eta$ D-wave S-matrix elements.

using the denominator of the resonance part of amplitude in the form

$$T^{res} = \sqrt{s}\Gamma_{el}/(m_{res}^2 - s - i\sqrt{s}\Gamma_{tot}).$$

Then

$$m_{res} = \sqrt{E_r^2 + (\Gamma_r/2)^2}, \quad \Gamma_{tot} = \Gamma_r. \tag{6}$$

The obtained values of the m_{res} and Γ_{tot} are shown in Table IV. It is clear that the values of these quantities, calculated from the pole positions on various sheets, mutually slightly differ; for the $f_2(2240)$ and $f_2(2410)$, lying in the energy region where data are very scanty, even considerably. We show only the values which match best the corresponding values M_r and the quantities $\sum_{i=1}^{N} f_{ri}^2/M_r$. The sheets on which the poles, used in calculation of m_{res} and Γ_{tot}, lie are also indicated. If two sheets are indicated, the pole positions on these sheets do not differ more than 1-1.5 MeV.

TABLE III: The f_2-resonance poles on sheets II, IV, VIII, and XVI for eleven states. $\sqrt{s_r} = E_r - i\Gamma_r/2$ in MeV is given.

	II		IV		VIII		XVI	
State	E_r	$\Gamma_r/2$	E_r	$\Gamma_r/2$	E_r	$\Gamma_r/2$	E_r	$\Gamma_r/2$
$f_2(1270)$	1282±2.6	67.5±4.2	1257±3.5	99.6±3	1277±3	73.4±4	1264±3.4	98±3.5
$f_2(1430)$	1425±48	98.8±54	1421±49	109±53	1426±48	98±55	1422±49	109±52
$f_2'(1525)$	1534±13	24±28	1534±13	23±9	1534±13	17±29	1534±13	19.5±28
$f_2(1600)$	1590±44	80.5±34	1592±41	74±34	1600±41	23±35	1601±40	9.4±35
$f_2(1710)$	1710±12	87±27	1711±11	84±27	1717±9.6	42.4±27	1718±9	32±27
$f_2(1810)$	1752±26	79±15	1752±26	84±15	1757±25	50.6±15	1758±25	36.5±15
$f_2(1960)$	1958±43	50±19	1957±43	57±19	1962±42	3.5±19	1962±42	7.4±19
$f_2(2000)$	2003±36	84±62	2004±35	68±64	2003±35	82±64	2002±36	95±62
$f_2(2020)$	2025±39	52±51	2026±38	45.4±57	2026±38	42.5±57	2025±39	52±51
$f_2(2240)$	2196±62	103±54.5	2197±62	98±55	2202±61	24±57	2201±62	45±57
$f_2(2410)$	2385±49	71±58	2387±47	5.6±61	2387±48	18.7±60	2385±49	84±59

TABLE IV: The masses and total widths of the f_2-resonances (all in MeV)

	$f_2(1270)$	$f_2(1430)$	$f_2'(1525)$	$f_2(1600)$	$f_2(1710)$	$f_2(1810)$
m_{res}	1268.0±3.4	1425.5±49.2	1533.8±13.4	1592.3±44.3	1712.2±11.6	1753.8±25.6
Γ_{tot}	196.0±7.0	218.6±105.4	48.4±56.0	161.0±68.6	174.0±53.8	167.6±29.4
Sheet	XVI	IV, XVI	II, IV	II	II	IV
	$f_2(1960)$	$f_2(2000)$	$f_2(2020)$	$f_2(2240)$	$f_2(2410)$	
m_{res}	1958.0±42.9	2004.0±36.3	2026.0±39.0	2198.8±62.3	2386.0±48.7	
Γ_{tot}	113.6±37.0	189.2±123.2	104.4±102.2	205.6±109.0	167.6±117.0	
Sheet	IV	XVI	II, XVI	II	XVI	

IV. ANALYSIS OF THE ISOVECTOR F-WAVE OF $\pi\pi$ SCATTERING

In analysis of the $\pi\pi$-scattering data in the $I^G J^{PC} = 1^+ 3^{--}$ sector by B. Hyams et al. [7], we took into account that the dominant modes of decay of the $\rho_3(1690)$ are $\pi\pi$, 4π, $\omega\pi$, $K\overline{K}$ and $K\overline{K}\pi$, and therefore have used the four-channel Breit–Wigner forms in

constructing the Jost matrix determinant $d(\sqrt{s-s_1}, \sqrt{s-s_2}, \sqrt{s-s_3}, \sqrt{s-s_4})$ where s_1, ..., s_4 are, respectively, the thresholds of the first four channels given above. The resonance poles and zeros in the S-matrix are generated by the Le Couteur–Newton relation

$$S_{11} = d(-\sqrt{s-s_1}, \cdots, \sqrt{s-s_4})/d(\sqrt{s-s_1}, \cdots, \sqrt{s-s_4}) \ . \tag{7}$$

The resonance part (2) of the d-function has the form

$$d_{res}(s) = \prod_r \left[M_r^2 - s - i \sum_{j=1}^{4} \left(\sqrt{\frac{s-s_j}{M_r^2-s_j}} \right)^7 R_{rj} \ f_{rj}^2 \right] \ . \tag{8}$$

The Blatt–Weisskopf factor for a particle with $J = 3$ is

$$R_{rj} = \frac{15 + 3(\sqrt{M_r^2-s_j}\ r_{rj})^2 + \frac{2}{5}(\sqrt{M_r^2-s_j}\ r_{rj})^4 + \frac{1}{15}(\sqrt{M_r^2-s_j}\ r_{rj})^6}{15 + 3(\sqrt{s-s_j}\ r_{rj})^2 + \frac{2}{5}(\sqrt{s-s_j}\ r_{rj})^4 + \frac{1}{15}(\sqrt{s-s_j}\ r_{rj})^6} \tag{9}$$

with radii of 0.927 fm in all channels as the result of the analysis.

The background part (3) turned out to be elastic:

$$d_B = \exp\left[-i \left(\sqrt{\frac{s-4m_\pi^2}{s}} \right)^7 a_1 \right] \tag{10}$$

where $a_1 = -0.0138 \pm 0.0011$.

In the analysis we considered the cases with one and two resonances. We obtained a good description in both cases: the total $\chi^2/\text{NDF} \approx 1$. In Figure 3 we show results of our fitting to the data for the case of two resonances.

The obtained parameters of the Breit–Wigner forms and the generated poles on the relevant sheets are shown in Tables V and VI, respectively.

TABLE V: The parameters of the Breit–Wigner forms for two ρ_3-like states (all in MeV).

State	M_r	f_{r1}	f_{r2}	f_{r3}	f_{r4}
$\rho_3(1690)$	1707.8±13.7	284.4±15.9	435.3±21.0	208.6±18.4	113.5±25
$\rho_3(1950)$	1833.5±28.6	96.3±18.3	331.8±28.0	297.7±16.5	110.4±28.3

Finally, in Table VII we show the mass and total width of the $\rho_3(1690)$ and its branching ratios compared with the average values from the PDG tables.
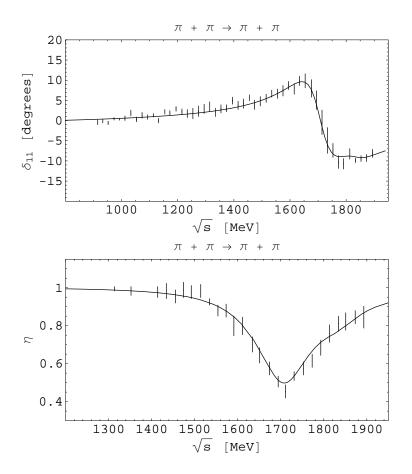
FIG. 3: The phase shift and module of the $\pi\pi$-scattering F-wave S-matrix element.

TABLE VI: The poles, generated by the Breit–Wigner forms on sheets II, IV, VIII, and XVI. $\sqrt{s_r} = \mathrm{E}_r - i\Gamma_r/2$ in MeV is given.

	II		IV		VIII		XVI	
State	E_r	$\Gamma_r/2$	E_r	$\Gamma_r/2$	E_r	$\Gamma_r/2$	E_r	$\Gamma_r/2$
$\rho_3(1690)$	1705±5.6	48±8	1707.6±4.5	15.3±13	1703.6±3.9	70±14	1700.5±4.4	87.7±13.5
$\rho_3(1950)$	1830.4±28	55±14	1833.5±29	0.0±22.7	1833.5±27.5	11.7±15	1831±24.3	53.3±22.3

V. DISCUSSION AND CONCLUSIONS

- In the $I^G J^{PC} = 0^+ 2^{++}$ sector, we carried out two analyses – without and with the $f_2(2020)$. We did not obtain $f_2(1640)$, $f_2(1910)$, $f_2(2150)$ and $f_2(2010)$, however, we saw $f_2(1430)$ and $f_2(1710)$ which are related to the statistically-valued experimental points.

- Usually one assigns the states $f_2(1270)$ and $f_2'(1525)$ to the first tensor nonet. One

11

TABLE VII: The parameters of the $\rho_3(1690)$ and its branching ratios compared with the average values from the PDG tables.

Scenario	m_{res} [MeV]	Γ_{tot} [MeV]	$\Gamma_{\pi\pi}/\Gamma_{tot}$	$\Gamma_{\pi\pi}/\Gamma_{4\pi}$	$\Gamma_{K\overline{K}}/\Gamma_{\pi\pi}$	$\Gamma_{\omega\pi}/\Gamma_{4\pi}$	$\Gamma_{K\overline{K}}/\Gamma_{tot}$
1 state	1703 ± 4	179 ± 12	0.29 ± 0.022	0.472 ± 0.097	0.146 ± 0.06	0.235 ± 0.04	0.042 ± 0.03
2 states	1702.7 ± 4	175 ± 11	0.271 ± 0.021	0.427 ± 0.096	0.159 ± 0.045	0.23 ± 0.04	0.043 ± 0.032
PDG	1688.8 ± 2.1	160 ± 10	0.243 ± 0.013	0.332 ± 0.026	$0.118^{+0.039}_{-0.032}$	0.23 ± 0.05	0.013 ± 0.0024

could assign the $f_2(1600)$ and $f_2(1710)$ states to the second nonet, though the isodoublet member is not discovered yet. If $a_2(1730)$ is the isovector of this octet and if $f_2(1600)$ is almost its eighth component, then from the GM-O formula

$$M_{K_2^*}^2 = \frac{1}{4}(3M_{f_2(1600)}^2 + M_{a_2(1730)}^2),$$

one would expect this isodoublet mass at about 1633 MeV. In the relation for masses of nonet

$$M_{f_2(1600)} + M_{f_2(1710)} = 2M_{K_2^*(1633)},$$

the left-hand side is only by 1.2% larger than the right-hand one.

In Ref. [15], one has observed the strange isodoublet in the mode $K_s^0\pi^+\pi^-$ with yet indefinite remaining quantum numbers and the mass 1629 ± 7 MeV. This state could be the tensor isodoublet of the second nonet.

• The states $f_2(1963)$ and $f_2(2207)$ together with the isodoublet $K_2^*(1980)$ could be put into the third nonet. Then in the relation for masses of nonet

$$M_{f_2(1963)} + M_{f_2(2207)} = 2M_{K_2^*(1980)},$$

the left-hand side is only by 5.3% larger than the right-hand one.

If one considers $f_2(1963)$ as the eighth component of octet, the GM-O formula gives $M_{a_2} = 2030$ MeV. This value coincides with that for the a_2 meson obtained in analysis [16]. This state is interpreted [2] as the second radial excitation of the 1^-2^{++} state based on consideration of the a_2 trajectory on the (n, M^2) plane where n is the radial quantum number of the $q\bar{q}$ state.

- As to the $f_2(2000)$, the presence of the $f_2(2020)$ in the analysis with eleven resonances helps to interpret $f_2(2000)$ as the glueball. In the case of ten resonances, the ratio of the $\pi\pi$ and $\eta\eta$ widths is in the limits obtained in Ref. [2] for the tensor glueball on the basis of the $1/N_c$-expansion rules. However, the $K\overline{K}$ width is too large for the glueball. In both, practically the same, descriptions of the processes, the parameters of f_2 states do not differ too much, except for the $f_2(2000)$ and $f_2(2410)$. The mass of the latter has decreased by about 40 MeV but the $K\overline{K}$ width of the former has changed significantly. Now all the obtained ratios of the partial widths are in the limits corresponding to the glueball.

  The question of interpretation of the $f_2(2020)$ and $f_2(2410)$ is open.

- Finally we have $f_2(1430)$ and $f_2(1710)$ which are neither $q\bar{q}$ states nor glueballs. Since one predicts that masses of the lightest $q\bar{q}g$ hybrids are bigger than those of lightest glueballs, these states might be the 4-quark ones. Then for the isodoublet mass of the corresponding nonet, we would expect the value 1570-1600 MeV. For now we do not know any experimental indications for the tensor isodoublet of that mass. However, in the known experimental spectrum of the K_2^* family, there is a 500-MeV unoccupied gap from 1470 to 1970 MeV [1], except for the above work [15]. Moreover, as one can see in the PDG tables on the $a_2(1700)$ listing, widths of the observed isovector tensor states in the 1660-1775-MeV interval differ by the factor 2-3, i.e., the states possess various properties. For example, the broad state with mass 1702 ± 7 MeV and width 417 ± 19 MeV, observed in $\bar{p}p \rightarrow \eta\eta\pi^0$ [17], might be the isovector member of the corresponding four-quark nonet.

  Of course, an assumption of this possibility presupposes an existence of the scalar tetraquarks at lower energies [18] which are not seen in our analysis [3]. One can argue that these states are a part of the background due to their very large widths.

- The analysis of the F-wave $\pi\pi$ scattering data by B. Hyams et al. [7] indicates that, except for the known $\rho_3(1690)$ (in our analysis $m_{res} \approx 1703$ MeV, $\Gamma_{tot} \approx 175$ MeV), there might be one more state lying above 1830 MeV. Since the $\pi\pi$ scattering data above 1890 MeV are absent, it is impossible to say something conclusive on parameters of this state. However, the $\rho_3(1950)$ does not contradict to the data but instead improves a little bit the obtained parameters of the $\rho_3(1690)$ and its branching ratios when

comparing them with the PDG tables [1].

[1] K. Nakamura *et al.* (PDG), J. Phys. G **37**, 075021 (2010).

[2] V.V. Anisovich *et al.*, Int. J. Mod. Phys. A **20**, 6327 (2005).

[3] Yu.S. Surovtsev, P. Bydžovský, R. Kamiński and M. Nagy, Phys. Rev. D **81**, 016001 (2010).

[4] Yu.S. Surovtsev, T. Branz, T. Gutsche and V.E. Lyubovitskij, Physics of Particles and Nuclei **41**, 990 (2010).

[5] S. Godfrey and N. Isgur, Phys. Rev. D **32**, 189 (1985).

[6] Yu.S. Surovtsev and P. Bydžovský, Frascati Phys. Series **XLVI**, 1535 (2007); Nucl. Phys. A **807**, 145 (2008).

[7] S.D. Protopopescu *et al.*, Phys. Rev. D **7**, 1279 (1973); B. Hyams *et al.*, Nucl. Phys. B **64**, 134 (1973); P. Estabrooks and A.D. Martin, Nucl. Phys. B **79**, 301 (1974).

[8] I. Yamauchi and T. Komada, Frascati Phys. Series **XLVI**, 445 (2007).

[9] N.M. Budnev *et al.*, Phys. Lett. B **70**, 365 (1977).

[10] S.B. Gerasimov and A.B. Govorkov, Z. Phys. C **13**, 43 (1982); **29**, 61 (1985); E. van Beveren, G. Rupp, T.A. Rijken and C. Dullemond, Phys. Rev. D **27**, 1527 (1983).

[11] J. Blatt and V. Weisskopf, *Theoretical nuclear physics*, Wiley, N.Y., 1952.

[12] D. Krupa, V.A. Meshcheryakov and Yu.S. Surovtsev, Nuovo Cimento A **109**, 281 (1996).

[13] K.J. LeCouteur, Proc. Roy. Soc. A **256**, 115 (1960); R.G. Newton, J. Math. Phys. **2**, 188 (1961).

[14] S.J. Lindenbaum and R.S. Longacre, Phys. Lett. B **274**, 492 (1992); R.S. Longacre *et al.*, Phys. Lett. B **177**, 223 (1986).

[15] V.M. Karnaukhov *et al.*, Yad. Fiz. **63**, 652 (2000).

[16] A.V. Anisovich *et al.*, Phys. Lett. B **452**, 173 (1999); **452**, 187 (1999); **517**, 261 (2001).

[17] I. Uman *et al.* (FNAL E835), Phys. Rrev. D **73**, 052009 (2006).

[18] R.L. Jaffe, Phys. Rev. D **15**, 267, 281 (1977); N.N. Achasov *et al.*, Phys. Lett. B **96**, 168 (1980); Z. Phys. C **22**, 53 (1984).